Transactions of the Materials Research Society of Japan 26 [4] 1291-1294 (2001)

Observation of Interactions between Condensable Gas Atom and Substrate from Optical Emission

Nariaki Imamura, Jun Sakaguchi, Syu-ichiro Asatani and Kozo Obara
Kagoshima University, Korimoto 1-21-40, Kagoshima 890-0065, Japan
Fax: 81-099-285-8401, e-mail: eem9308@elib.eee.kagoshima-u.ac.jp

We present effects of the interaction between condensable gas atoms and walls in plasma derived from temperature dependence of emission spectra. Intensities of emission spectra from Hg atoms exponentially increased as temperature increased. Below 310 K, the activation energy of the group A (370, 579 nm) and that of the group B (404, 435 and 546nm) was 0.45 eV and 0.67 eV, respectively. The activation energy of the group B coincided with that of evaporation from mercury surface. Above 310 K, the activation energy of the group B decreased to 0.34 eV, which is a half of the energy of evaporation from the surface of liquid mercury. The *dT/dt* dependence of the activation energy for mercury below 310K approached to the activation energy for liquid phase mercury as the rate *dT/dt* decreased. This result suggests a structural change of adsorbed mercury atoms from multi-layer to monolayer. Time dependence of emission spectra induced by temperature perturbation with amplitude 1 K and period 800 s was investigated. Below 310 K, the behaviors of Xe, Ar and Hg were correlated. However, above 310 K, the correlation between them was changed; high harmonic modes were remarkably excited in both cases, but second harmonic mode of Xenon spectrum disappeared.

Key words: condensation, mercury, adsorption, evaporation, dissipation

1. INTRODUCTION

Monitoring the surface state of the substrate is a key to proceed the crystal growth process and synthesis of new materials. On crystal growth with plasma processes, input energy is dissipated by the following processes; the excitations and the ionization of neutral molecules, mass and thermal transfer of gaseous species, light emission from meta-stable atoms. Finally the input energy is dissipated to the substrate and the walls as thermal energy, and then the crystal grows on the substrate. Temperature near the substrate influences the plasma near the walls through the evaporation and adsorption of the atoms on the substrate, and is an important factor to influences the formation and size distribution of crystal on the substrate. At the present time, condensation processes of sputtered particles in microscopic viewpoints are not clear because of the shortage of microscopic measurements of the processes [1].

On the other hand, the collision processes in plasma are most important keys for developing the light source device. For saving the consumed energy, it is important to improve the emission. The energy dissipation processes in the discharge cell dominate these keys. In the case of light source device with mercury vapor, the states of the evaporation and adsorption of mercury atoms on the walls decide the mercury vapor pressure in the cell, and the emission intensity and efficiency of the cell depend on the mercury vapor pressure.

In this paper, we present time and spatial dependence of emission spectra from plasma with mercury, argon and xenon atoms in periodic temperature perturbation.

2. EXPERIMENT

A thin flat type discharge cell with 17.4x12.4x1.6 mm^3 was used for measuring two-dimensional behaviors of mercury atoms [2]. Total pressure in the cell was 40 Torr (Ar:Xe=4:1). Ar pressure was 32 Torr and Xe pressure was 8 Torr. The total mass of mercury in the cell was about 1 mg. Input power was supplied by inverter-type power source with repetition frequency 13.25 kHz, pulse width 1 μs, pulse voltage 700 V and pulse current 40 mA. Emission spectra were measured by multi-channel spectrometer with an optical fiber. The range of analyzed wavelength was from 330 nm to 850 nm. Temperature of the cell was controlled by an electric heater, which installed under thick copper plate, from room temperature to 470 K. Spatial distributions of emission spectra were measured by using optical fiber system of diameter 0.4 mm and X-Y stage with precision 1 μm. Mercury is only one condensable element in the system. The behaviors of gaseous species were monitored by their inherent emission spectra. Temperature dependence of emission spectra from plasma was measured for long periods, max. 30 hours, to investigate the interaction with long time constants.

Temperature perturbation with amplitude 1 K, was added to investigate the dynamic effects of boundary conditions of the wall. The frequency dependence of the fluctuated emission intensity induced by periodic temperature perturbation was analyzed by FFT method. For investigating the condensation state of mercury in non-equilibrium condition, temperature of the cell was changed with a constant rate.

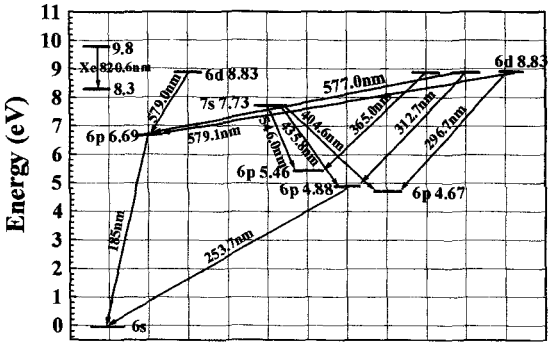

Fig.1 The energy diagram of mercury and xenon

3. THEORETICAL MODEL

The intensity emitted from plasma is correlated with the density of constituent elements in the gas phase. We assume that the intensities emitted from meta-stable constituent atoms are proportional to the concentration in the plasma [3]. The dominant emission lines are 365 nm, 404 nm, 435 nm, 546 nm and 579 nm from mercury and 820 nm from [4]. The emitted line from argon atoms was neglected because of low intensity, which act as a particle for collisional quenching. The energy diagram of these emission lines is shown in Fig.1.

The excitation for the emitting species in plasma is performed by electron impact.

$$X+e \rightarrow X^*+e, \qquad \text{rate constant } k_e \tag{1}$$

where X^* is the excited state of X atom, and e is electron. De-excitation process can come about in radiative decay and collisional quenching.

$$X^* \rightarrow X+h\nu, \qquad \text{rate constant } k_r \tag{2}$$

$$X^*+M \rightarrow X+M+(\text{kinetic energy of } M), \qquad \text{rate constant } k_q \tag{3}$$

where h and ν are the Planck constant and the frequency of emitted light, respectively. $[X^*]$, the concentration of X^*, is equal to the summation of the concentrations of radiative decay and collisional quenching from the mass balance at steady-state of plasma. Then $[X^*]$ can be expressed as follows [5],

$$[X^*] = \frac{k_e[X][e]}{k_r + k_q[M]} \tag{4}$$

From equation (2), the intensity of the optical emission is given as follows,

$$I \propto k_r[X^*] = \frac{k_e[X][e]}{1+(k_q/k_r)[M]} \tag{5}$$

The energy transfer from the excitation atom to X atom of ground state can occur as follow,

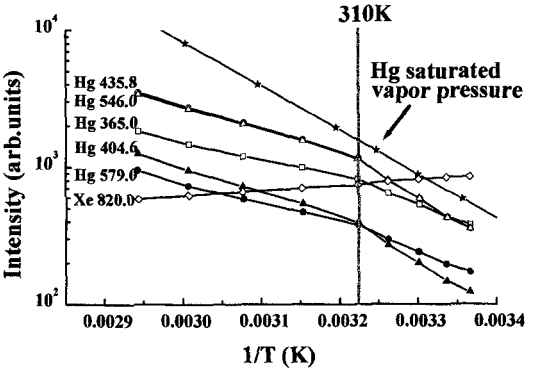

Fig.2 The temperature dependence of emission spectra. The activation energy was classified into two groups. The value changed at 310 K.

$$X+M^* \rightarrow X^*+M+(\text{kinetic energy of } M), \qquad \text{rate constant } k_M \tag{6}$$

In this case, the reaction rate is proportional to $k_M[M][X]$. At steady state of plasma, we can assume that the concentration of mercury atoms in vapor is in the local equilibrium with adsorbed mercury on the substrate at temperature T.

$$[X] \propto N\exp\left(-\frac{E_X}{kT}\right) \tag{7}$$

where N is the number of adsorbed mercury sites with activation energy E_X for evaporation, and k is Boltzmann constant. Considering the equation (5) and (7), the intensity for emitting mercury atoms reflects the adsorbed state of mercury atoms on the substrate.

4. EXPERIMENTAL RESULTS

Figure 2 shows temperature dependence of emission spectra for mercury and xenon atoms. The logarithmic emission intensity was proportional to the inverse of temperature. The gradients of each emission line changed at 310 K We estimated the activation energy, E_X, from the temperature dependence of the intensity. The activation energy was classified in two groups. Emission lines from mercury atoms at 365nm and 579 nm (group A) showed activation energy 0.45 eV below 310 K, and 0.24 eV above 310 K, respectively. Emission lines from mercury atoms at 404 nm, 435 nm, 546 nm (group B) showed activation energy 0.67 eV below 310 K, and 0.34 eV above 310 K, respectively.

The profile of the emission intensity of xenon showed perfectly different from that of mercury, which showed negative correlation with the emission intensity of mercury. The activation energy estimated from emission intensity from xenon was –0.1 eV.

The activation energy of mercury in liquid phase estimated from its saturated vapor pressure showed 0.64eV in the whole temperature region of this experiment, as shown in Figure 2. The activation energy of the group B is approximately equal to that of mercury saturated vapor pressure.

Figure 3 shows the dT/dt dependence of the activation energy, which was estimated from temperature dependence of emission intensity of mercury 546 nm below 310K at constant dT/dt. The activation energy

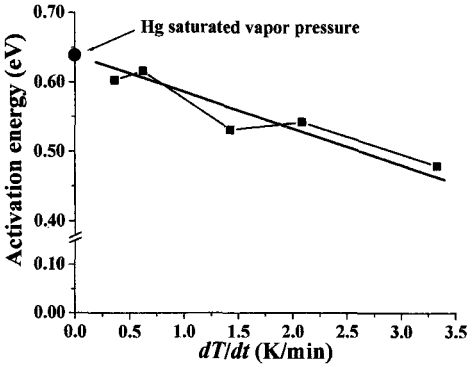

Fig.3 The *dT/dt* dependence of the activation energy. The activation energy approached to the activation energy of liquid phase Hg, as the rate *dT/dt* decreased.

for the mercury emission intensity approached to the activation energy estimated from temperature dependence of saturated vapor pressure of mercury as the rate *dT/dt* decreased.

Figure 4 (a) and 4 (b) show typical time dependence examples of the emission intensity for mercury 546 nm and xenon 820 nm at 297 K and 338 K under the periodic temperature perturbation, respectively. The period of temperature perturbation was 800 s and its amplitude ΔT was 1 K. At 297 K, time dependence of the intensity from mercury 546 nm and xenon 820 nm was roughly correlated with each other at the peak of emission intensity as shown figure 4 (a). At 338 K, time dependence of the intensities from mercury 546nm and xenon 820 nm became more complex as shown figure 4 (b). They were negatively correlated with each other.

Figure 5 (a) and 5 (b) show the results of FFT estimated from data in figure 4 (a) and 4 (b), respectively. At 297 K, frequency dependence of emission intensities from mercury 546 nm and xenon 820 nm were correlated with the temperature fluctuation with 0.00134 Hz, as shown in figure 5 (a). However, at 338 K, the amplitudes of higher harmonic modes increased in both emission lines mercury 546 nm and xenon 820 nm, as shown in figure 5 (b). The frequency of the fundamental mode decreased from 0.00134 Hz at 297 K to 0.00125 Hz at 338 K. The amplitude of the second harmonic mode in xenon 820 nm at 338 K remarkably decreased as compared with the intensity at 297 K.

Below 310 K, spatial distribution of emission intensity at mercury 546 nm showed 2x3 mode and that of xenon 820 nm showed a different mode close to 1x3. As temperature increased, spatial distribution relatively became smooth[2].

5. DISCUSSION

In the following discussions, we suppose that the rate constants k_e, k_r, k_q, and k_q for the reaction equations (1), (2), (3) and (6) are constant in the temperature range; 300 K < T < 350 K.

In the temperature dependence of emission spectra, the coincidence with the activation energy of the

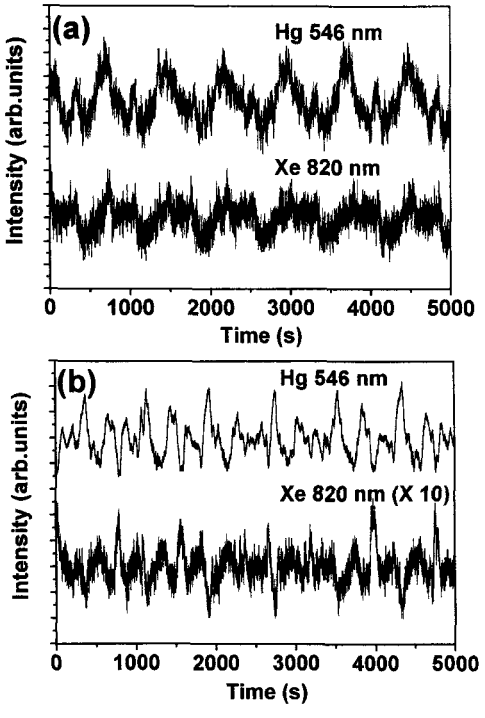

Fig.4 The time dependence of emission intensity under the periodic temperature perturbation, ΔT=1 K. (a) and (b) was measured at 297 K and at 338 K, respectively.

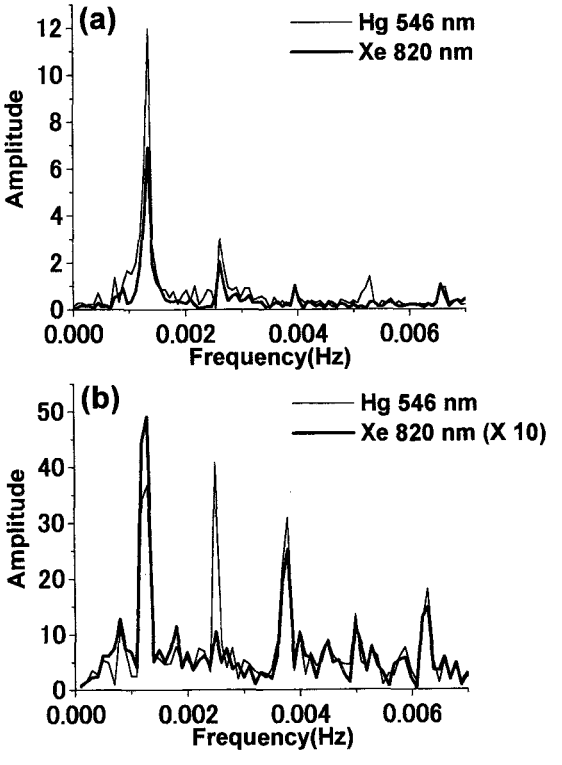

Fig.5 FFT results estimated from data in Fig.4. (a) and (b) were results at 297 K and at 338 K, respectively.

emission intensity for the group B (404 nm, 435 nm, 546 nm of mercury) below 310 K and the latent heat of mercury evaporation from liquid surface supports the validity of this assumption. This result shows that mercury atoms was condensing like droplets below 310 K. Considering the reaction rate of equation (6) and the temperature dependence of emission intensity of equation (7), the difference between the activation energy, 0.45 eV, of the group A (365 nm , 579 nm of mercury) and the activation energy, 0.67 eV, of the group B (404 nm, 435 nm, 546 nm of mercury) can be explained by the energy transfer from exited xenon atoms to the meta stable species of the group A of mercury. As shown in Fig. 1, The energy level of the excited state of the group A, 8.83 eV, is lower than the energy level 9.8 eV of that of Xe 820 nm, and higher than the energy of the final state of light emission Xe 820 nm [6]. However, the energy level of the excited state of the group B, 7.73 eV, is lower than the energy level of the final state of light emission Xe 820 nm. Then the exited Xe atoms, which radiate the light emission of 820 nm, preferentially excite the group A, and the group B was basically exited by electron impacts.

Above 310 K, the decrease of the activation energy for Hg (404 nm, 435 nm, 546 nm) suggest the reduction of the number of bonds of evaporating mercury atoms on the substrate. As the temperature increases, the condensation state of mercury shifts from the most stable three dimensional nucleation, two dimensional nucleation. In this model we can explain the decrease of the activation energy above 310 K by the reduction of the number of the bonds from six bonds deduced from the effective state in three dimensional liquid case to three bonds for the corner of the hexagonal plate in two dimensional nucleation. The activation energy of the evaporation from two-dimensional condensation state was deduced as a half 0.32 eV of that of liquid mercury 0.64 eV. This value approximately corresponds with the activation energy for the group B above 310 K.

The decrease of activation energy with increasing the rate of temperature change suggests the change of the number of evaporation sites, N in equ. (7). N is proportional to the number of mercury islands. From nucleation theory, if we apply the model that mercury evaporate from the corners of island, N is proportional to $\exp(-\Delta G/kT)$, where G is free energy for formation of nucleation. As ΔG is negative for growing islands, logarithm of emission intensity is proportional to $\exp[-(Ex - \Delta G)/kT]$. Then, since ΔG is proportional to super-saturation $\Delta\mu$, ΔG is proportional to dT/dt in linear approximation. Therefore, the activation energy is proportional to dT/dt.

The time dependence of emission intensity under temperature perturbation was related to the dynamics of the interactions between evaporated mercury atoms and excited atoms. Below 297 K, the intensity from xenon 820 nm was higher than that from mercury atoms. This showed the concentration of mercury atoms was smaller than that of xenon atoms. The time correlation between the emission intensities from mercury and xenon corresponds to each other. This result shows that, below 310 K, gas system is in thermal equilibrium state with the external thermal sources, which dominates the fluctuation of light emission.

Above 310 K, the increase of higher harmonic modes became strong. This is because the structural change of mercury atoms on the substrate, which causes the decrease of activation energy, and induces rapid evaporation of mercury.

6. CONCLUSION

The Activation energy estimated from temperature dependence of emission spectra was classified into two groups, group A (365 nm, 579 nm) and group B (404 nm, 435 nm, 546 nm). The activation energy of the group A was approximately equal to the activation energy from liquid mercury. However, that of group B was smaller than that of the group A, because the energy transfers from exited xenon atoms due to the atomic collisions.

The rate of temperature change influenced the activation energy of emission spectra. As dT/dt decreased, the activation energy approached to that of liquid mercury. This experimental fact was explained by using the nucleation theory and by assuming that mercury atoms were evaporated from corner of islands.

The decrease of activation energy at $T > 310$ K suggests the change of the condensation state of mercury atoms on the substrate. The time dependence of emission spectra induced by temperature fluctuation suggested the interactions between Hg and excited Xe which were related to the evaporation and the adsorption of mercury on the substrate. The remarkable decrease of second harmonics of emission intensity from Xe 820 nm seems to be a key to solve the microscopic interaction between Hg and Xe near the surface or electrode.

Finally, we conclude that, in the thin flat cell, we can clarify the signal of the interaction between condensable atoms and the substrate surface from temperature dependence of optical emission spectra.

ACKNOWLEDGEMENTS

The authors thank to Mr. M.Sarata and Mr. A.Honda for preparing glass discharge cells and to Prof.N.Terada, Prof.T.Hirose an Prof.S.Hirooka for helpful discussions.

REFERENCE

[1] K.Obara, P.Yiji, Y.Suemoto, T.Ogushi and W.Möller, Vacuum, 51 (1998) 491

[2] K.Obara, N.Imamura, J.Sakaguchi, R.Higashizono, Display, 21(2000) 105

[3] S.K.Wu, Y.S.Chen, J.Z.Chen, Thin Solid Films 365 (2000) 61

[4] G.Herzberg, Atomic Spectra and Atmic Structure (Dover Publication, New York, 1994)

[5] R.d'Agostino, F.Cramarossa, V.Colaprico and R.d'Ettole, J.Appl.Phys., 54 (1983) 1284

[6] B.Eliasson, B.Gellert, J.Appl.Phys.68 (1990) 2026

(Received December 7, 2000; Accepted January 31, 2001)